

Fatigue behaviour of mullite studied by the indentation flexure method

P. Hvizdoš^a, M.J. Reece^{b,*}, R. Torrecillas^c

^a*Institute of Materials Research, Slovak Academy of Sciences, Košice, Slovakia*

^b*Queen Mary and Westfield College, University of London, Mile End Road, London, UK*

^c*CSIC Instituto del Carbon, Oviedo, Spain*

Received 25 October 1999; received in revised form 25 May 2000; accepted 4 June 2000

Abstract

A systematic study has been performed of the use of the Indentation Flexure Fatigue (IFF) method to study crack growth in mullite at room temperature and high temperature (1300°C). The results obtained for a mullite have been compared with previous data generated on the same material, but using the more direct compact tension method. The material produces transgranular crack growth and consequently does not show R-curve behaviour, which considerably simplifies the comparison of the data generated by both methods. The IFF method can significantly overestimate the crack tip stress intensity factor because of the way in which the residual stress intensity produced by the indentation is estimated. The experimental details that influence the test results were investigated. © 2000 Elsevier Science Ltd. All rights reserved.

Keywords: Crack growth; Fatigue; Indentation; Mechanical properties; Mullite

1. Introduction

The types of tests that have been used to study subcritical crack growth behaviour in ceramics fall into two categories: those based on the growth of long, induced cracks (>100 µm); and those based on short, natural flaws (<100 µm). The experiments involving long cracks enable the direct observation of the growing cracks and the evaluation of the velocity of the crack, v , as a function of the applied stress intensity factor, K . While those using short, and usually unobservable cracks, involve either long term tests to measure the time-to-failure under static and cyclic stresses or the effect of subcritical behaviour on the strength of specimens stressed at different rates, in what are known as “dynamic” fatigue experiments. The results of tests performed using unobservable natural flaws are subject to the influence of the statistical nature of the distribution and size of the flaw population, whereas in long crack experiments the statistical variation in data results primarily from direct measuring errors.

Experiments with long cracks can be performed by the direct loading of any specimen geometry that allows the stable initiation and growth of a crack. The tests are often performed using crack line loaded specimens, such as, double torsion,^{1–3} double cantilever beam^{1,2,4,5} or compact tension (CT),⁶ where cracks can be grown over distances greater than 1 mm. The fracture and fatigue behaviour of shorter cracks (<1 mm) has been studied in flexure using the indentation method to produce controlled surface cracks.^{7–10} All of these types of specimen geometries have been useful in elucidating the static and cyclic fatigue behaviour of ceramics.^{1–14}

The major disadvantage of using long cracks is that they may not behave in the same way as short, natural flaws. This is in fact the case in coarse grained materials, which produce crack bridging in the wake of the crack front, caused by the elastic and frictional contact of fractured grains.^{15–17} This leads to stress shielding of the crack-tip and, therefore, an apparent increase in the fracture toughness of the material. This effect has been well documented, and is now commonly referred to as Crack Resistance-curve or ‘R-curve’ behaviour because of the increase in fracture toughness with increasing crack length.^{15–17} In a coarse grained alumina (~16 µm grain size) the fracture toughness saturates at ~6 MPa

* Corresponding author.

E-mail address: m.j.reece@qmw.ac.uk (M.J. Reece).

$m^{1/2}$, which is about double its short crack value.¹⁸ Whilst this is an impressive increase in fracture toughness in a material, it should be realised that the critical flaws in these experiments were much larger (> 1 mm) than would be encountered in real components.

Experiments involving the direct observation of fatigue cracks can be very difficult and time consuming to perform. It is often difficult to nucleate stable cracks. The cracks are then highly sensitive to the crack tip stress intensity factor, K . The majority of the experimental methods involve specimen geometries that produce increasing K with crack growth, so that the crack growth is highly unstable. These problems are overcome when using the indentation flexure fatigue method (IFF).^{19,20} It involves introducing indentation flaws, which are then forced to grow by an applied flexural loading. The plastic zone associated with the indents produce residual tensile stresses on the cracks that decrease as they grow. This results in desirable stable crack growth over relatively long distances. The disadvantage of the method is that the residual stresses have to be accounted for in the analysis, leading to potential errors. Another advantage of the IFF method is that the cracks used are typically 100–500 μm long and are therefore relatively short and more typical of natural flaws.

The purpose of this study was to systematically investigate the limitations and errors associated with the use of the IFF method at room temperature and high temperature (1300°C). To do this the work was performed on a previously well characterised (microstructurally and mechanically) mullite material for which fatigue crack growth data, obtained using the compact tension method, already existed.^{21–23} Also, the material produces transgranular crack growth and consequently does not show R-curve behaviour, which considerably simplifies the comparison of the data generated by both methods. The IFF experiments were performed under identical testing conditions (temperature, frequency and load ratio) as those used in the CT experiments so that a direct comparison of the results obtained using the two different methods could be made.

2. Experiments and theory

2.1. Material

The material was prepared by sintering of a commercial mullite powder (Baikowski SA 193 CR) at 1750°C and for 5 h.^{21–23} During cooling from the sintering temperature, the samples were held for 5 h at 1450°C in order to reduce the content of amorphous phase. The resulting microstructure of the material consisted of a mixture of equiaxed and elongated grains with an average

size of ~ 4 μm and an aspect ratio from 1 to 5. The basic characteristics are shown in the Table 1. Sintered samples were machined and supplied in the form of plates with dimensions of $4 \times 25 \times 45$ mm.

2.2. Experimental methods

Bending bars were cut from the plates. Because the values of bending strength and fracture toughness were known to be relatively low, the dimensions of the bending bars were chosen to be $6 \times 4 \times 45$ mm, with the height being 6 mm in order to maximise the loading forces required to break the specimens. Two specimens were tested at each temperature (room temperature and 1300°C). Vickers indents of 5, 10, 15 and 20 kg were introduced within the inner spans on the tensile surfaces of all of the test bars. Two indentations for each load were made, making a total of eight for each specimen. The mechanical tests were carried out using an Instron 8511 servohydraulic machine. The testing equipment for the high temperature tests consisted of an alumina push-rod and an alumina four-point flexure jig with fixed rollers with 40/20 mm spacing. The flexure jig was enclosed in a furnace capable of achieving 1500°C.²²

2.2.1. Fracture toughness

The fracture toughness of the material was measured using Single Edge V-Notch Beam method (SEVNB) on three flexure bars according to the procedure as evaluated by the European Structural Integrity Society / Technical Committee 6 (ESIS/TC6).²⁴ The V-notch was prepared to a radius of ~ 10 μm by polishing with a razor blade covered with 0.25 μm diamond paste. The notched specimens were broken at a cross-head speed of 0.5 mm/min. Values of fracture toughness were calculated using the following formula²⁵

$$K_{IC} = \frac{F}{B\sqrt{W}} \frac{S_1 - S_2}{W} \frac{3\sqrt{\alpha}}{2(1-\alpha)^{1.5}} \gamma \quad (1)$$

where

$$\gamma = 1.9887 - 1.326\alpha - \frac{(3.49 - 0.68\alpha + 1.35\alpha^2)\alpha(1-\alpha)}{(1+\alpha)^2},$$

B is the specimen thickness, W is the of specimen height, S_1 and S_2 are the outer and inner spans (40/20 mm), respectively, α is the normalized notch depth (a/W), and F is the fracture load.

Table 1
Characteristics of the mullite material²¹

Density (g cm^{-3})	Estimated porosity (vol.%)	Estimated glass (vol.%)	Bend strength (MPa)
2.948	2.94	2	259

2.2.2. Fatigue tests

Fatigue tests were carried out using the indentation flexure method. The tensile surfaces were polished down to a 1 μm diamond paste finish. The indents were aligned so that their radial cracks were parallel and perpendicular to the long axis of the specimen. The plastic zone produced beneath the indent impressions produces a residual stress intensity factor, K_{res} , on the surface radial cracks that drives them to their equilibrium length. Using a semi-empirical analysis, the “indentation fracture toughness” can be estimated from measurements of these cracks:^{26,27}

$$K_{IC} = K_{res} = \eta \sqrt{E/H} \frac{P}{c^{3/2}} \quad (2)$$

where η is a geometric factor, E is the modulus of elasticity of the material, H is its Vickers hardness, P is the indentation load used, c is the indentation radial crack half-length at the surface. Fig. 1a shows the variation of K_{res} as a function of crack length.

The applied stress intensity factor at the tip of a crack on the tensile surface of a loaded bending bar is given by:

$$K_{app} = Y\sigma\sqrt{\pi a} \quad (3)$$

where σ is the stress applied on the tensile surface:

$$\sigma = \frac{3}{2} F \frac{(S_1 - S_2)}{BW^2}, \quad (4)$$

a is the crack depth, calculated using an ASTM suggestion:²⁸

$$a/W + a/c = 1, \quad (5)$$

and Y is a geometric factor which was calculated according to the finite-element analysis of Newman and Raju²⁹ for semielliptical surface cracks as a function of the surface crack length, c , crack depth, a , and specimen height, W . This relationship was investigated in this study and found to be accurate.

At room temperature the total stress intensity factor, K_{tot} , at the crack tip of the indentation crack subjected to bending was calculated as the sum of the residual stress and the applied stress:

$$K_{tot} = K_{res} + K_{app} = \eta \sqrt{E/H} \frac{P}{c^{3/2}} + Y\sigma\sqrt{\pi a}. \quad (6)$$

Fig. 1b schematically illustrates the applied, residual, and total stress intensity factors as functions of crack length for an ideal test. The profile of the K_{tot} curve illustrates the main advantage of the indentation flexure method, the fact that it can produce stable crack

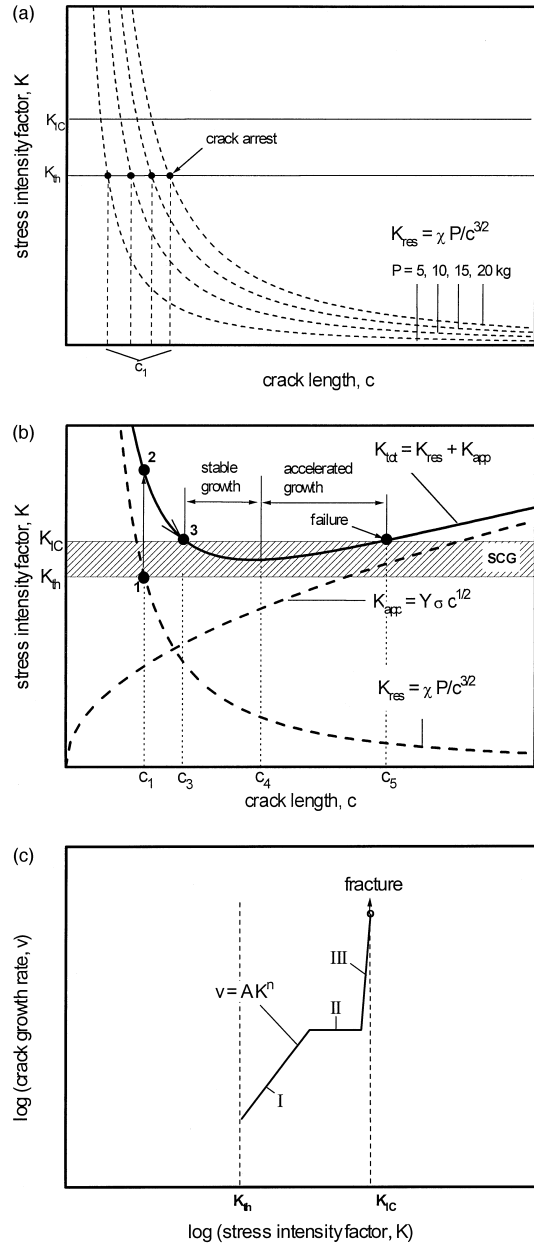


Fig. 1. (a). Residual stress intensity factor for indentation cracks in mullite produced by different loads. (b). Applied, residual, and total stress intensity factors at crack tip for an idealised indentation fatigue test as functions of the crack length. (c). Idealised v - K fatigue data for ceramic material.

growth. After indentation a radial crack will achieve an arrested/equilibrium length of c_1 and $K_{tot} = K_{res}$. This will not occur immediately because the final stage of crack growth is achieved by subcritical crack growth (SCG). By applying a bending load a crack can be made to grow. The K_{tot} may exceed K_{IC} and the crack will propagate rapidly, “pops-in”, to length c_3 . The crack will then grow stably to length c_4 , after which it will grow with increasing velocity to c_5 where it achieves a critical length resulting in fracture of the specimen. If the indents are chipped during indentation, as some-

times occurred in this work, the analysis of their crack growth is complicated by the fact that the residual stress is relaxed by some unknown amount.³⁰

Fig. 1c shows an idealised subcritical crack growth behaviour for a ceramic material.^{1,4} There may be some threshold value of stress intensity, K_{th} , below which a crack will not grow. If such a threshold does exist it would be difficult to prove because crack growth rates below 10^{-10} ms^{-1} are difficult to measure practically. Of the three different regions, I, II and III, the most significant in terms of time to failure of components is region I. In regions II and III the crack growth rates are typically $\geq 1 \times 10^{-5} \text{ ms}^{-1}$, and once the cracks are growing at these sorts of rates the specimens break very quickly. Therefore, it is usually the fatigue crack growth behaviour in region I that is of most interest and studied. In order to describe the subcritical crack growth behaviour in region I the empirical power law relation, so-called Paris' law, between the stress intensity factor, K , and the crack growth rate, v , is used:

$$v = \frac{da}{dt} = AK^n \quad \text{for } K > K_{th} \quad (7)$$

where A and n are constants which can be calculated from $\log v - \log K$ plot, and K_{th} is a threshold value below which no crack growth occurs.

After indentation, the crack lengths were measured at least one day later so that we could be sure that they had reached their equilibrium lengths. Then the specimens were subjected to their chosen test bending stress for 30 s. This allowed the cracks to pop-in. Depending on the testing conditions and the initial crack lengths, the cracks typically grew by 0–30 μm during pop-in. Following pop-in the new crack lengths were measured. The specimens were then reloaded and the actual fatigue test begun. This procedure meant that only crack growth associated with subcritical behaviour was studied and that no overestimate of the crack velocity was made as a consequence of including the pop-in growth. The testing was stopped periodically (usually after ~ 1 h) to measure the crack growth.

The measurements of the crack lengths were made using an optical microscope. The corresponding K was estimated as the average of the K_{tot} for the initial and final crack lengths. The average crack propagation velocity was calculated by dividing the crack elongation by the test duration. If after a series of measurements a specimen was not broken and the velocity of the crack propagation became too low (usually less than 10^{-10} ms^{-1}), a new higher bending stress was chosen and testing was continued again after the initial pop-in procedure. The cyclic tests were conducted with a sinusoidal waveform at a test frequency, f , equal to 1 Hz, and a load ratio $R = K_{min}/K_{max} = 0.1$. Values of K_{max} were used to plot the v - K data for the cyclic tests. The crack

growth rates under static loading, da/dt , and cyclic loading, da/dN , can be compared using:

$$\frac{da}{dt} = \frac{da}{dN} f. \quad (8)$$

The high temperature fatigue behaviour of mullite was studied at 1300°C . The temperature was chosen to coincide with test conditions used in the previous studies.^{21,22} At this temperature significant glass softening occurs. The specimens were heated to the test temperature at a rate of $15^\circ\text{C min}^{-1}$. During heating the specimens were pre-loaded at 20 N ($\sim 5 \text{ MPa}$) to reduce the possibility of crack healing. After reaching the test temperature, the specimens were allowed to anneal for 1 h and then loaded and tested for 1 h. The purpose of the annealing was to attempt to remove the residual stresses associated with the indents.

Following the mechanical tests, the fracture surfaces and fracture paths of the surface and subsurface fatigue cracks were studied using scanning electron microscope (JEOL JSM-6300) with the aim of identifying the fracture and fatigue damage mechanisms.

3. Results and discussion

3.1. Room temperature

The Vickers hardness of the mullite was $9.0 \pm 0.4 \text{ GPa}$. The fracture toughness value measured by SEVNB method was $2.0 \pm 0.2 \text{ MPa m}^{1/2}$. This is consistent with a previous measurement of $2.3 \pm 0.2 \text{ MPa m}^{1/2}$ obtained using the compact tension method.^{21,22} This result enabled us to calibrate the material and geometry constants used in Eq. (2). A series of Vickers indentations were made on the polished surface of a specimen. The indentation loads were 5, 7.5, 10, 15, 20 and 27.5 kg. From the slope of the $c^{3/2}$ vs P graph in Fig. 2, the value of $\chi = \eta\sqrt{E/H} = 0.069$ was obtained.

The elimination of the initial popping was essential for the correct determination of the crack growth rate. For example, after applying a bending load of 20 MPa on a crack produced using an indentation load of 5 kg, the initial pop in measured after 30 s was 8 μm ($\sim 5\%$ of its original length), after which the crack did not grow anymore, whereas a crack produced with a 20 kg indentation load under the same bending condition grew by 25 μm ($\sim 7\%$ of its original length), and this was approximately the same elongation as the total crack growth that took place during the 60 min test that followed. The magnitude of K_{app} was dependent on the applied load and crack length, and was typically between 0.3 and 1.1 $\text{MPa m}^{1/2}$.

The results of the fatigue tests at room temperature are plotted in Fig. 3. The full squares and the full

triangles represent the static and cyclic data respectively. The two sets are coincident within the scatter of the data. The same observation was made previously for the same material when studied using the compact tension method.^{21,22} The crack growth rates in some polycrystalline ceramics that show R-curve behaviour at room temperature are, however, significantly greater under cyclic loading compared to static loading.^{6,11,12} This is a consequence of the cyclic loading producing closure forces on the crack faces, which damage the crack bridging ligaments. The explanation for the different behaviour of the mullite appears to be that because it had a predominantly transgranular fracture path (Fig. 4),²¹ it did not produce significant crack bridging and R-curve behaviour, and was therefore not susceptible to mechanical fatigue. This is supported by the observation that the K_{IC} (SEVNB) and CT data (see Fig. 3)^{21,22} are consistent, although they were generated for very different crack lengths. Additionally, it was found in the CT work that the crack opening displacements were not hysteretic and the compliance of the

specimens fitted the theoretical estimates, also suggesting that crack bridging was not significant.²¹

3.2. Chipped indents

The hollow squares in Fig. 3 denote results obtained from indents for which the surface around the impression had chipped (Fig. 5). The cracks associated with the chipped indents tended to exhibit lower crack growth velocities compared to the unchipped indents. This is probably due to the fact that the chipping partially relaxed the residual stress because the plastic zone becomes less constrained. To investigate this behaviour further, indents were purposely chipped by repeatedly loading the same indentation impression.³⁰ The specimen was then tested under static loading using the same method as previously and the results are shown in Fig. 6. The data has been plotted twice, with the crack stress

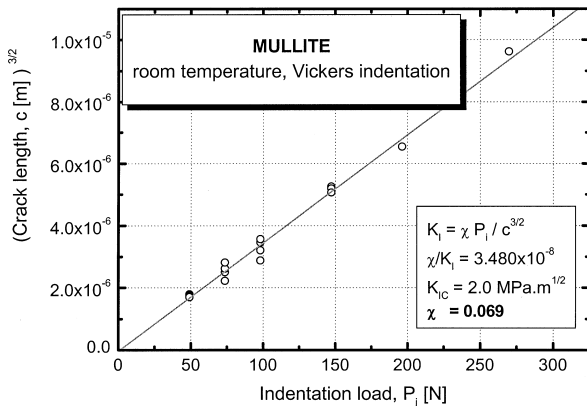


Fig. 2. Indentation crack length as a function of indentation load.

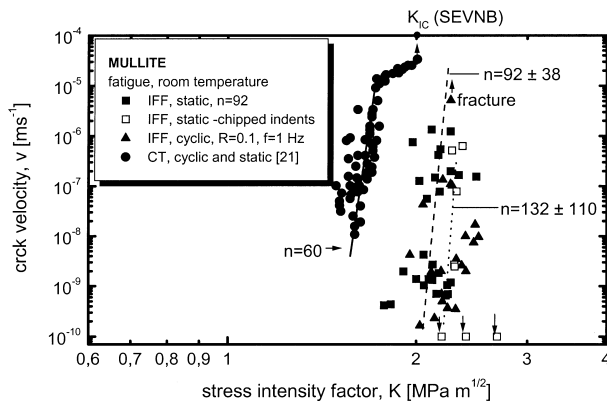


Fig. 3. v - K data for mullite at room temperature obtained using the indentation fatigue method. The solid line data was obtained using the compact tension method²¹ and was drawn through overlapping cyclic and static data.

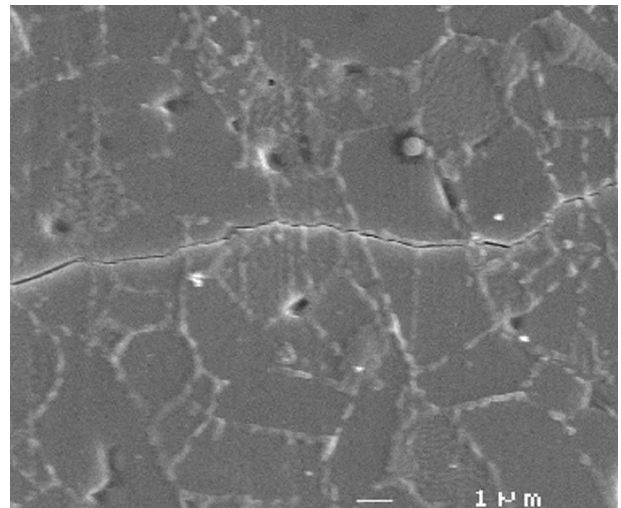


Fig. 4. SEM micrograph of the fracture path at room temperature.

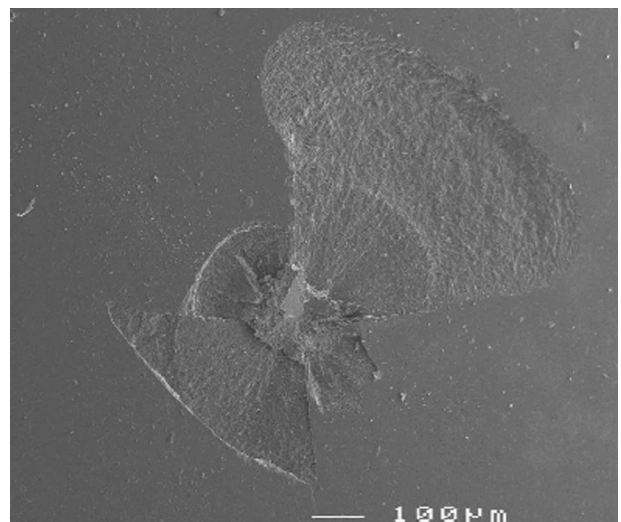


Fig. 5. Chipped indent.

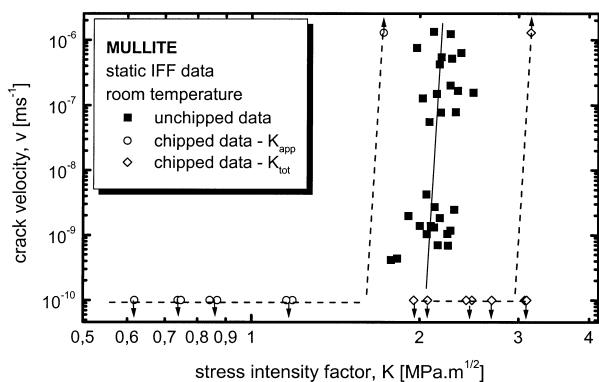


Fig. 6. Static fatigue crack growth data for indents that have been chipped on purpose by repeated indentation. The stress intensity has been plotted as K_{app} , assuming that $K_{res} = 0$, and K_{tot} , assuming that K_{res} has its full value. For comparison data for unchipped indents is shown.

intensity estimated as K_{tot} and also as K_{app} (assuming $K_{res} = 0$). Because K_{res} was significantly reduced, the crack growth was very unstable and it was not possible to generate complete subcritical crack growth data. This illustrates very well the usefulness of the indentation fatigue method in enabling stable crack growth under normal conditions, when the indentation residual stress is relatively large. Also included in Fig. 6 is the static fatigue crack growth data for unchipped indents. Comparison of the different sets of data suggests that the residual stress was reduced by $\sim 60\%$ due to the chipping. The use of repeated indentation therefore, unfortunately, does not provide a simple method for completely removing the indentation residual stress. If it did, it would have provided an interesting approach to producing “controlled” flaws for fracture toughness testing using indentation flexure fracture toughness methods.³¹ The results for chipped indentations does, however, have some significance for the scratching, point impact and wear of ceramics. In terms of reducing the propagation of surface radial and subsurface median cracks, which limit the strength of ceramics, it may be better if point contact damage is accompanied by chipping. A good example of this has been observed in the case of scratch damage on glazes.³² It was found that the visual damage initially increased with increasing load. However, at a relatively high level of load, the visual damage then began to decrease. The explanation was that at the higher loads a trough of material, including the plastic zone, was gouged out at the point contact. The removal of the plastic zone resulted in removal of the associated residual stresses and consequently the radial/median cracks were much shorter than they would have been. This produced a significant reduction in the visual damage of the glazes.

3.3. Correction of data

Fig. 3 shows the fatigue crack growth for mullite obtained using the compact tension method in the

previous study.²¹ The data line also represents a best fit through the combined static and cyclic data. The differences in the slopes of the CT and IFF data, although large, are not significant considering the scatter of the data. There is, however, a significant displacement of the IFF data to higher K 's compared to the CT data. This appears to be a typical feature of the IFF method. An explanation for this systematic overestimating of K by the IFF method seems to be that, according to the commonly used Eq. (2), the residual stress intensity factor at the equilibrium / arrested crack length is taken to be equal to the critical values (K_{IC}), but in fact it must be equal to K_{th} . Therefore the magnitude of the overestimate of K values can be calculated as equal to $K_{IC} - K_{th}$. We can make a crude estimate of the overestimate by arbitrarily assuming that K_{IC} and K_{th} in Fig. 3 correspond to extrapolated crack velocities of 10^{-4} and 10^{-10} ms^{-1} , respectively. In which case, the overestimate of K is ~ 0.26 $\text{MPa m}^{1/2}$. The IFF data in Fig. 3 has been corrected and replotted in Fig. 7. This correction improves the correlation of the IFF and CT data, it also makes the IFF data consistent with the SEVNB data. The Corrected IFF data and CT data differ by only 0.2 $\text{MPa m}^{1/2}$. This difference is possibly a consequence of the limiting precision of determining v and K in the two methods. For instance, the difference is similar to the magnitude of the error of measuring of the fracture toughness using the SEVNB method (2.0 ± 0.2 $\text{MPa m}^{1/2}$).

3.4. High temperature

The IFF method is potentially very useful for investigating crack growth at high temperature because of its simplicity compared to other methods. Fig. 8 shows a comparison of static fatigue crack growth data at 1300°C for the IFF and CT methods. The IFF data has been plotted as K_{tot} and K_{app} (assuming $K_{res} = 0$). At 1300°C the glassy intergranular phase in the mullite was above its softening temperature ($\sim 1200^\circ\text{C}$), and annealing of the residual stresses was anticipated. We are unable to quantify by how much this has occurred. If we assumed that the corrected results for the IFF method would be similar to those obtained by the CT method, then, despite the pretest anneal for 1 h at 1300°C before the fatigue tests, the residual stresses were only partially removed. Further support for this suggestion is given by the behaviour of chipped indents. They were not observed to grow (Fig. 8). This suggests that the chipping further reduced residual stresses that must have therefore been present. This uncertainty in the magnitude of the residual stress is a recurring problem when using the IFF method for high temperature testing. To overcome the problem it is commonly assumed that some annealing treatment will remove the residual stresses and simplify the analysis. However, our

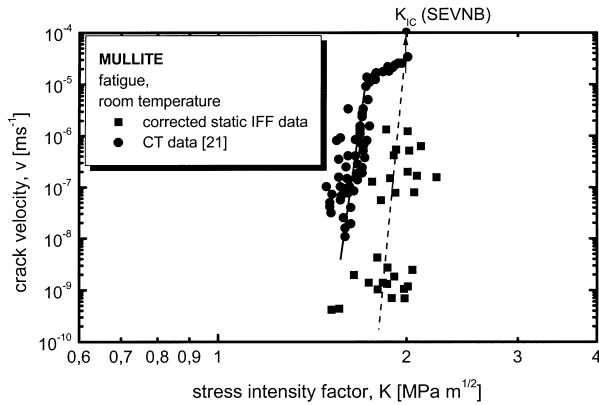


Fig. 7. Corrected indentation flexure data at room temperature compared with compact tension data.²¹

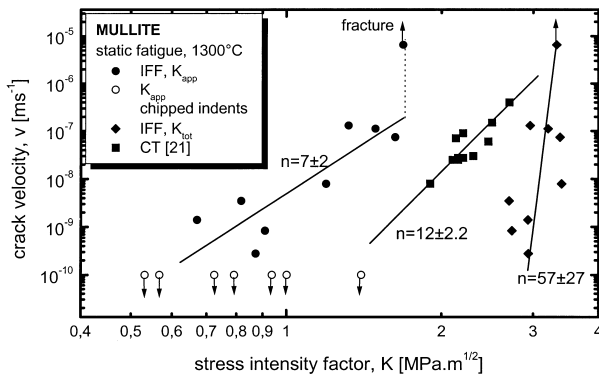


Fig. 8. High temperature static fatigue data showing comparison of compact tension data²¹ and indentation flexure data.

results importantly suggest that even annealing well above the glass softening temperature may not be sufficient. Comparing the behaviour of complete indents with purposely chipped indents may provide a qualitative means of determining whether any annealing treatment has significantly reduced the residual stress.

The fractographic study of the crack paths showed that the fatigue crack growth at 1300°C had both transgranular and intergranular character with occasional crack deflection and bridges formed by the glassy phase (Fig. 9). The study of the fracture surfaces showed a clear difference between the fatigue and the fast fracture surfaces. The latter one was distinctly more transgranular in character, and more similar to the room temperature crack paths.

3.5. Estimation of a

The different fracture behaviour for fatigue crack growth and fast fracture at high temperature enabled us to investigate the subsurface crack shape (Fig. 10). This was not possible at room temperature because the two fracture surfaces were not distinguishable. The ASTM suggestion²⁸ of calculating the crack depth, a , [Eq. (5)],

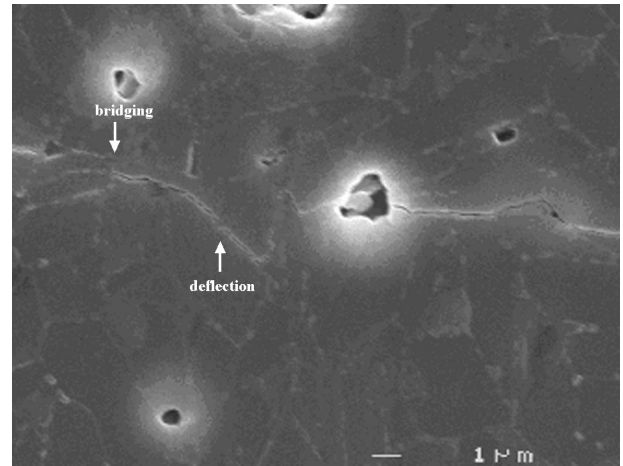


Fig. 9. Crack deflection and bridging of cyclic fatigue crack at 1300°C.

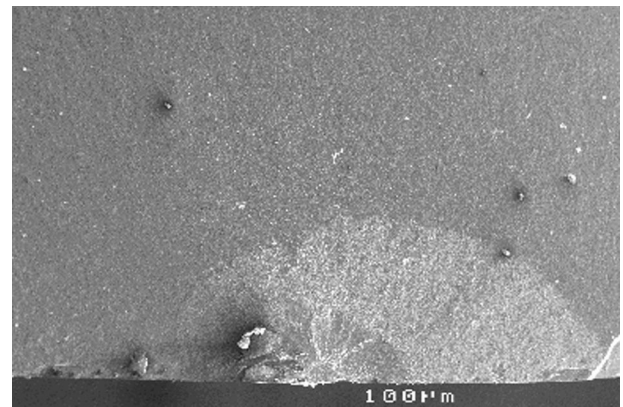


Fig. 10. Fracture surface of specimen tested under static fatigue loading at 1300°C. Visible are indentation crack, and regions of the fatigue and fast crack growth.

produces a reasonably good estimate for the present material. The ratio $a_{\text{measured}}/a_{\text{calculated}}$ was 0.85 for the indentation crack and 0.91 for the final dimensions of the fatigue crack which caused the failure. The error associated with this estimate gives some idea of the limiting precision of the measurement of v - K data. The error associated with estimating a alone can give rise to a significant fraction of the difference between the corrected IFF data and the CT in Fig. 7. A 15% error in the estimate of a alone would result in a 8% error in the estimate of K_{app} .

4. Conclusions

The indentation flexure fatigue method is a relatively fast, simple and inexpensive method for studying directly the growth of fatigue cracks. It produces stable crack growth.

The method as it is commonly used, tends to overestimate the crack tip stress intensity factor. We believe this is due to a common assumption that the equilibrium/arrested indent cracks are subject to a stress intensity factor equal to the critical value (K_{IC}), whereas in fact they are subjected to the smaller, crack growth threshold value, K_{th} .

Corrected IFF data for mullite at room temperature shows a reasonably good fit to CT data considering the scatter and errors always inherent in fatigue experiments.

The chipping of indents produced a significant reduction of the indentation residual stresses (~60%) at room temperature.

The IFF method is particularly useful for studying fatigue crack growth under difficult conditions, such as for materials with large stress exponents, or studying materials at high temperatures.

Heat treatment above the glassy phase softening temperature may not completely remove the indentation residual stresses, as is sometimes assumed.

The uncertainty in the analysis of the data and the scatter of the data for the IFF method limits its usefulness. However, considering its practical advantages over other methods, it provides an excellent method for investigating the effect of loading conditions on fatigue crack growth. It also, provides a good method for comparing the fatigue behaviour of different materials.

Acknowledgements

This work was supported by the Royal Society NATO Fellowship, which financed stay of P. Hvizdoš at QMW College, London. We would also like to thank F. Guiu, C. K. L. Davies, G. Fantozzi and C. Olagnon for their discussions during the Brite-Euram project. We would particularly like to thank M. Li who generated the fatigue crack growth data during the Brite-Euram project.

References

1. Wiederhorn, S. M., Freiman, S. W., Fuller, E. R. and Simmons, C. J., Effects of water and other dielectrics on crack growth. *J. Mater. Sci.*, 1982, **17**, 3460–3478.
2. Evans, A. G. and Lange, F. F., Crack propagation and fracture in silicon carbide. *J. Mater. Sci.*, 1975, **10**, 1659–1664.
3. Evans, A. G., A method for evaluating the time-dependent failure characteristics of brittle materials and its application to polycrystalline alumina. *J. Mater. Sci.*, 1972, **7**, 1137–1146.
4. Wiederhorn, S. M., Influence of water vapour on crack propagation in soda-lime glass. *J. Am. Ceram. Soc.*, 1967, **50**, 407–414.
5. Michalske, T. A. and Bunker, B. C., Stress corrosion of ionic and mixed ionic/covalent solids. *J. Am. Ceram. Soc.*, 1986, **69**, 721–724.
6. Dauskardt, R. H., Marshall, D. B. and Ritchie, R. O., Cyclic fatigue-crack propagation in magnesia-partially-stabilized zirconia ceramics. *J. Am. Ceram. Soc.*, 1990, **73**, 893–903.
7. Hoside, T., Ohara, T. and Yamada, T., Fatigue crack growth from indentation flaw in ceramics. *Int. J. Frac.*, 1988, **37**, 47–59.
8. Petrovic, J. J. and Jacobson, L. A., Controlled surface flaws in hot pressed SiC. *J. Am. Ceram. Soc.*, 1976, **59**, 34–37.
9. Sglavo, V. M. and Dal Maschio, R., Controlled indentation-induced cracks for the determination of fracture toughness in alumina. In *Frac. Mech. Of Ceramics. Vol. 11*, ed. R. C. Bradt et al. Plenum Press, New York, 1996, pp. 233–243.
10. Petrovic, J. J., Jacobsen, L. A., Talky, P. K. and Vasudevan, A. K., Controlled surface flaws in hot-pressed Si₃N₄. *J. Am. Ceram. Soc.*, 1975, **58**, 113–116.
11. Krohn, D. A. and Hasselman, D. P. H., Static and cyclic fatigue behaviour of polycrystalline alumina. *J. Am. Ceram. Soc.*, 1972, **55**, 208–211.
12. Reece, M. J., Guiu, F. and Sammur, M. F. R., Cyclic fatigue crack propagation in alumina under direct tension-compression loading. *J. Am. Ceram. Soc.*, 1989, **72**, 348–352.
13. Evans, A. G. and Fuller, F. R., Crack propagation in ceramic materials under cyclic loading conditions. *Met. Trans.*, 1974, **5**, 27–33.
14. Evans, A. G. and Linzer, M. I., High frequency cyclic crack propagation in ceramic materials. *Int. J. Frac. Mech.*, 1976, **12**, 217–222.
15. Swanson, P. L., Fairbanks, C. J., Lawn, B. R., Mai, Y.-W. and Hockey, B. J., Crack-interface grain bridging as a fracture resistance mechanism in ceramics: I, Experimental study on alumina. *J. Am. Ceram. Soc.*, 1987, **70**, 279–288.
16. Mai, Y.-W. and Lawn, B. R., Crack-interface grain bridging as a fracture resistance mechanism in ceramics: II, Theoretical fracture mechanics model. *J. Am. Ceram. Soc.*, 1987, **70**, 289–294.
17. Bennison, S. J. and Lawn, B. R., Role of interfacial grain bridging sliding friction in the crack-resistance and strength properties of nontransforming ceramics. *Acta Metall.*, 1989, **37**, 2659–2671.
18. Reichl, A. and Steinbrech, R. W., Determination of crack-bridging forces in alumina. *J. Am. Ceram. Soc.*, 1988, **71**, c299–c301.
19. Alcalá, J. and Anglada, M., Fatigue and static crack propagation in yttria-stabilized tetragonal polycrystals: Crack growth micro-mechanisms and precracking effects. *J. Am. Ceram. Soc.*, 1997, **80**, 2759–2772.
20. Zhan, G.-D., Reece, M. J., Li, M. and Calderon-Moreno, J. M., Cyclic fatigue crack growth behaviour in β -(Si–Al–O–N) at ambient and elevated temperatures. *J. Mater. Sci.*, 1998, **33**, 3867–3874.
21. Davies, C. K. L., Guiu, F., Li, M., Reece, M. J. and Torrecillas, R., Subcritical crack propagation under cyclic and static loading in mullite and mullite-zirconia. *J. Eur. Ceram. Soc.*, 1998, **18**, 221–227.
22. Development of High Temperature Fatigue, Creep and Thermal Shock Resistant Zircon and Mullite Zirconia Ceramics, Final Technical Report for Brite-Euram Project No. BRE2-CT94-0613, QMW, London, 1997.
23. Torrecillas, R., Calderon, J. M., Moya, J., Reece, M. J., Davies, C. K. L., Olagnon, C. and Fantozzi, G., Suitability of mullite for high temperature applications. *J. Eur. Ceram. Soc.*, 1999, **19**, 2519–2527.
24. Kübler J., Fracture Toughness of Ceramics Using the SEVNB Method; Round Robin. VAMAS Report No37, ISSN 1016-2186, published by EMPA Dübendorf, Switzerland, May 1999.
25. Srawley J. E., Gross B., In *Cracks in Fracture*, Am. Soc. Test. Mater., Spec. Tech. Publ., No.601, ASTM, Philadelphia, PA, 1976, pp. 559-579.
26. Lawn, B. R., Evans, A. G. and Marshall, D. B., Elastic/plastic indentation damage in ceramics: the median/radial crack system. *J. Am. Ceram. Soc.*, 1980, **63**, 574–581.

27. Anstis, G. R., Chantikul, P., Lawn, B. R. and Marshall, D. B., A critical evaluation of indentation techniques for measuring fracture toughness: I, Direct crack measurement. *J. Am. Ceram. Soc.*, 1981, **64**, 533–538.
28. ASTM Standard E 740-80, Standard recommended practice for fracture testing with surface-crack tension specimens. In *ASTM Annual Book of Standards*, Vol. 301, American Society of Testing and Materials, Philadelphia, PA, 1983, pp. 740-750.
29. Newman, Jr., J. C. and Raju I. S., Analysis of Surface Cracks in Finite Plates under Tension or Bending Loads, NASA Technical paper 1578, NASA December 1979.
30. Reece, M. J. and Guiv, F., Repeated indentation method. *J. Am. Ceram. Soc.*, 1990, **73**, 1004–1013.
31. Mizuno, M. and Okuda, H., VAMAS round robin on fracture toughness of silicon nitride. *J. Am. Ceram. Soc.*, 1995, **78**, 1793–1801.
32. Cronins, A., unpublished work at Queen Mary and Westfield College.